arXiv:2111.11688v2 [hep-th] 16 May 2022

Entanglement between two evaporating black holes

Akihiro Miyata[a] **Tomonori Ugajin**[b,c]

[a]*Institute of Physics, University of Tokyo, Komaba,*
Meguro-ku, Tokyo 153-8902, Japan

[b]*Center for Gravitational Physics, Yukawa Institute for Theoretical Physics, Kyoto University, Ki-*
tashirakawa Oiwakecho, Sakyo-ku, Kyoto 606-8502, Japan

[c]*The Hakubi Center for Advanced Research, Kyoto University, Yoshida Ushinomiyacho, Sakyo-ku,*
Kyoto 606-8501, Japan

E-mail: miyata@hep1.c.u-tokyo.ac.jp,
tomonori.ugajin@yukawa.kyoto-u.ac.jp

Abstract: We study a thermo-field double type entangle state on two disjoint gravitating universes, say A and B, with an eternal black hole on each. As was shown previously, its entanglement entropy of the universe A is computed by the generalized entropy on a new spacetime constructed by suitably gluing the black holes on A and B. We study such spacetime gluings when universes are asymptotically flat and AdS cases, especially when the masses of these black holes are different. We also clarify the rule to construct such a glued spacetime in more general settings from the gravitational path integral view point.

Contents

1 Introduction

The semi-classical description of a black hole and the Hawking quanta entangled with it has appeared to be inconsistent with principles of quantum theory in many respects [1, 2]. In particular, although the von Neumann entropy of the Hawking radiation should follow a Page

curve [3, 4] due to the unitarity of quantum theory, the naive von Neumann entropy of the Hawking radiation in the semi-classical description does not. Recent developments show that we can get the von Neumann entropy of the Hawking radiation R in a semi-classical way by using the so-called island formula [5–7],

$$S_{\text{island}}(\rho_R) = \underset{I}{\text{MinExt}} \left[\frac{\text{Area}(\partial I)}{4G_N} + S_{\text{eff}}(R \cup I) \right], \tag{1.1}$$

where $\text{Area}(\partial I)$ is the area of the endpoints of a new region I called the island, and $S_{\text{eff}}(R \cup I)$ is the von Neumann entropy of the bulk effective quantum field theory on the union of the two regions R and I, computed on a fixed background spacetime, and $\underset{I}{\text{MinExt}}$ denotes the extremization and the minimization of the generalized entropy over all possible islands I (see figure 1). The island contribution originates from so-called replica wormholes connecting different replicas in computing the von Neumann entropy of the Hawking radiation by using the replica trick in the semi-classical description of gravity [8, 9]. See also e.g., [10–65] for discussions on the island formula, and e.g., [66–72] on replica wormholes.
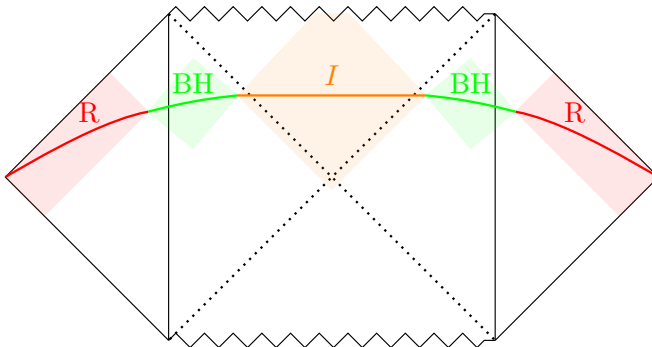
Figure 1: The Penrose diagram of an AdS black hole coupled to the non-gravitating external bath. We take the radiation region R (red solid line) in the non-gravitating external bath. After the Page time, the island region I (orange solid line) becomes non-empty, and the entanglement wedge of the black hole BH is outside the horizon of the black hole (green shaded region).

A frequently used setup for studying the von Neumann entropy of Hawking radiation consists of a black hole in anti-de Sitter (AdS) spacetime and a non-gravitating external bath system attached at the AdS boundary (see figure 1 again) with the transparent boundary conditions [5–7, 9, 73]. Using such a setup, we can actually get the Page curve by using the island formula.

The introduction of the non-gravitating bath helps to define the Hawking radiation R

without ambiguities coming from gravitational effects and simplifies the situation. However, if we consider a bath which is also gravitating, then the situation drastically changes and becomes more complex. Such setups are studied in [40], see also [48, 53, 54, 62]. However, there are subtle points in defining the von Neumann entropy in the presence of dynamical gravity. One of them is that the tensor factorization of Hilbert spaces associated with gravitating regions is not well-defined because of the existence of the gravitational edge modes living in the boundary of such regions [74], see also [75] for a recent discussion on the implication of this fact to the island formula. The other difficulty is that the diffeomorphism invariance of gravity does not allow us to define a region in an unambiguous way.

One way to avoid these subtleties is to prepare two disjoint gravitating universes A and B, then make them entangled [54][1]. In this setup, one can take the entangled state to be the thermo-field double state on the two universes

$$|\Psi\rangle = \sum_i \sqrt{p_i}|\psi_i\rangle_A \otimes |\psi_i\rangle_B, \quad p_i = \frac{e^{-\beta E_i}}{Z(\beta)}, \tag{1.2}$$

where $|\psi_i\rangle_{A,B}$ are bulk effective field theory eigenstates with energy E_i. We will study this state in detail in next section 2. In computing the entanglement entropy of the state on the universe A (or the universe B) by using the replica trick, the dominant replica wormhole contribution is the one connecting all the gravitating universe's replicas when the entanglement between the two universes is sufficiently large $\beta \to 0$ [54]. Such a contribution leads us to the formula,

$$S(\rho_A) = \text{Min}\{\text{S}_{\text{th}}(\beta), \ \text{S}_{\text{swap}}(\rho_A)\}, \quad \text{S}_{\text{swap}}(\rho_A) = \underset{\text{I}}{\text{MinExt}} \left[\frac{\text{Area}(\text{A/B}, \partial \text{I})}{4\text{G}_\text{N}} + \text{S}_{\text{eff}}(\text{I})\right], \tag{1.3}$$

where $\text{Area}(A/B, \partial I)$ is the area of ∂I on a new spacetime denoted by A/B, which is constructed by glueing two original universes A and B, and $S_{\text{eff}}(I)$ is the von Neumann entropy in the bulk quantum field theory of the region I on the new spacetime A/B (see figure 2). Also $S_{\text{th}}(\beta)$ denotes the thermal entropy of the same bulk QFT with the temperature $1/\beta$. The appearance of the new spacetime A/B comes from the above mentioned wormhole, and one can consider such a new spacetime A/B as a realization of the "ER=EPR" [76], which states that the existence of the entanglement between two distant regions is related to the existence of a wormhole connecting the two regions. In other words, the sufficiently large entanglement between the two disjoint universes A, B induces a geometric connection between them, leading to the introduction of the new spacetime A/B (see figure 2 again).

In the previous paper [54], only the simplest setup where the universes A, B have eternal black holes with the same black hole mass (or equivalently a same black hole entropy) was

---

[1]See also [48] for the related discussion, and [28, 29, 49] for the discussion on entangled two disjoint universes, one of which is non-gravitating and the other is gravitating and contains a black hole.
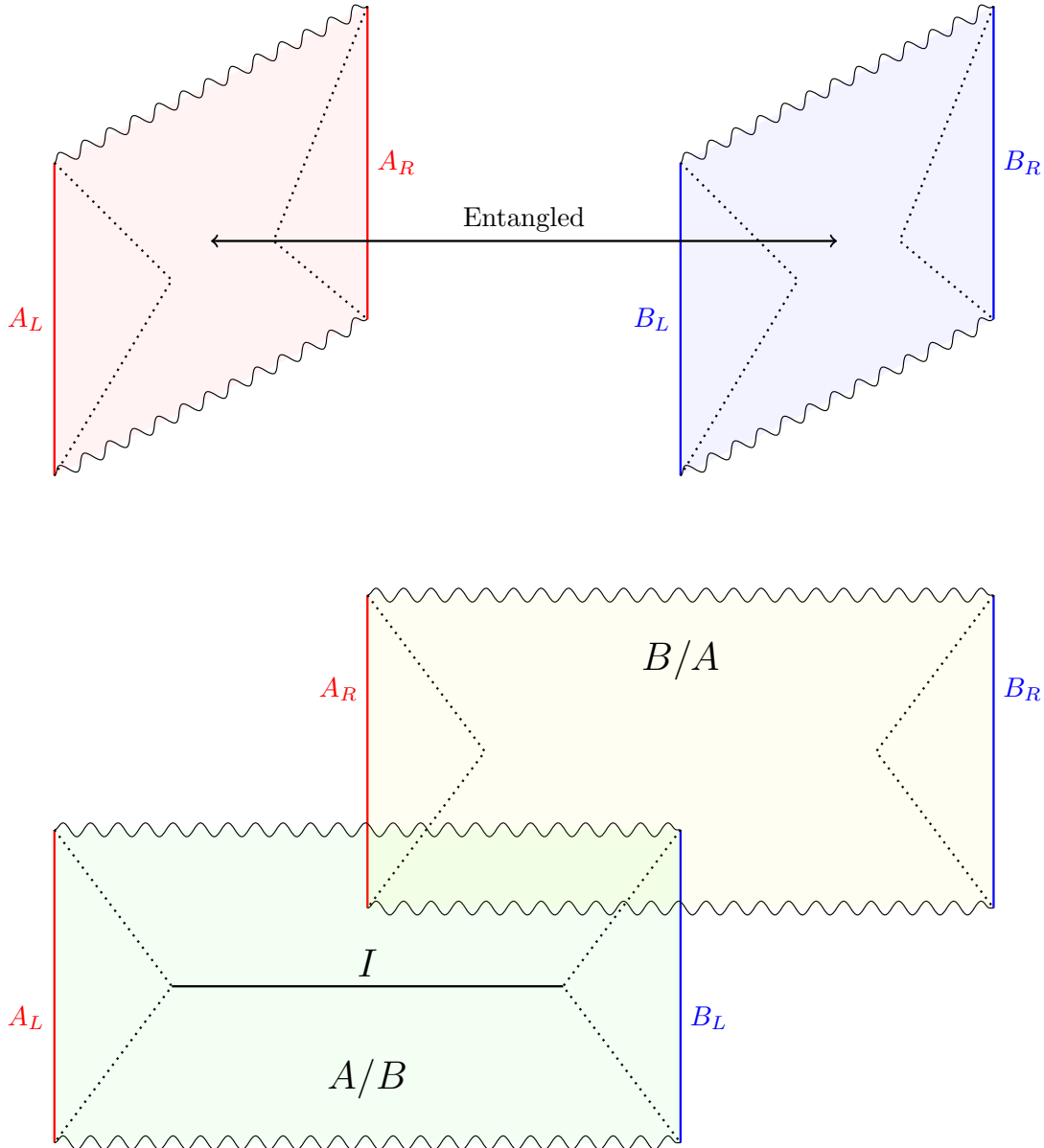
Figure 2: Schematic picture of two phases of entangled two universes (AdS) A, B. (Top) The two universes are disjoint and just entangled with each other. In this case, the entanglement entropy of the state (1.2) on the universe A is the Hawking-like thermal entropy $S_{\text{th}}(\beta)$. (Bottom) A sufficiently large entanglement between the two universes induces the geometric connection of the two spacetimes, resulting in two glued spacetimes A/B and B/A. Unlike the above disjoint universes, since there is an island in the glued spacetime A/B, the entanglement entropy of the universe A is given by the black hole entropy of the glued spacetime A/B.

studied. The resulting glued spacetime A/B also contains eternal black holes with the same mass.

In this paper, we generalize this entropy calculation, and discuss more involved setups where the black hole mass in the universe A is different from the one in the universe B, to further understand the detailed properties of the formula (1.3). In such situations, there are several possibilities for the glued geometry A/B, which are indistinguishable in the previous setup [54]. Our results show that the dominant glued geometry A/B, which contributes the entropy formula (1.3) is given by the one which minimizes the total black hole entropy in A/B. For definiteness, in this paper we focus on two dimensional dilaton gravities; Jackiw-Teitelboim gravity in two-dimensional AdS spacetime and CGHS gravity in two dimensional flat spacetime.

The outline of our paper is as follows. In section 2, we review and explain the results of the previous paper [54] on the entanglement entropy between two gravitating universes. In section 3, we construct a dilaton profile describing the glued spacetimes A/B with different black hole masses for AdS JT gravity, and in the next section 4 we do a similar construction for CGHS gravity. In section 5, by using the dilaton profiles constructed in previous sections we compute the von Neumann entropy of the universe A and give its interpretation. In section 6 we discuss an approximate way to construct such a glued geometry using shock waves. In section 7, we consider more general settings where the each of these two eternal black holes has different the left and the right black hole masses, $M_{AL} \neq M_{AR}, M_{BL} \neq M_{BR}$, for AdS JT gravity and for flat CGHS gravity, and then compute the entanglement entropy of the universe A. In section 8, we summarize our results and discuss their implications and future directions. In appendix A, we provide ADM mass formulae for AdS JT gravity and CGHS gravity. In appendix B, we explain another method to construct glued spacetimes approximately by using shock waves for AdS JT gravity, in appendix C we explain a similar method for CGHS gravity.

2 Entanglement between two gravitating universes

In this paper, we are interested in the following setup discussed in [54]. First, we prepare two disjoint gravitating universes, say A and B with the identical cosmological constant as in figure 2. Furthermore we assume A and B are described by a two dimensional dilaton gravity theory. For simplicity, we consider two dimensional AdS JT gravity

$$I_{\text{grav}}^{\text{AdS}} = -\frac{\phi_0}{16\pi G_N} \left[\int_D R + \int_{\partial D} 2K \right] - \frac{1}{16\pi G_N} \int_D \Phi(R - \Lambda) - \frac{\Phi_b}{16\pi G_N} \int_{\partial D} 2K, \qquad (2.1)$$

when the cosmological constant is negative, and CGHS gravity

$$I_{\text{grav}}^{\text{Flat}} = -\frac{1}{16\pi G_N} \int_{\mathcal{M}} (\Phi R - \Lambda) - \frac{1}{16\pi G} \int_{\partial\mathcal{M}} 2\Phi K, \tag{2.2}$$

when these two universes are asymptotically flat. In these theories, only the dynamical degree of freedom is the dilaton Φ, and we can always fix the metric part. We will especially discuss situations where each universe contains a two-sided eternal black hole. The eternal black hole in the universe A is specified by the dilaton profile Φ_A and we also have Φ_B for the black hole in B.

As a matter degrees of freedom coupled to the gravity degrees of freedom, we take a conformal field theory. We define it both of these universes A and B, so that the Hilbert space of the matter degrees of freedom is bipartite. On this Hilbert space, we take the following entangled CFT state,

$$|\Psi\rangle = \sum_{i=1}^{\infty} \sqrt{p_i} |\psi_i\rangle_A |\psi_i\rangle_B \quad p_i = \frac{e^{-\beta E_i}}{Z(\beta)}, \tag{2.3}$$

where $\{|\psi_i\rangle_A\}_{i=1}^{\infty}$ are energy eigenstates. We can safely assume that CFT_A on the universe A and CFT_B has the same spectrum $\{E_i\}_{i=1}^{\infty}$, because this conformal field theory only couples to the metric which is non-dynamical in theories of dilaton gravity.

This setup provides an ideal toy model to study the entanglement structure of evaporating black holes emitting Hawking radiation. Imagine an observer keeps collecting the Hawking quanta emitted from an evaporating black hole in some universe, say A. Then the observer sends these quanta to another universe, say the universe B, which means that the universe B plays a role of a bath collecting the Hawking quanta. This operation provides a concrete way to prepare the state (2.3) in question. Specifically, increasing $1/\beta$ corresponds to increase the entanglement in the radiation state (2.3). Thus, this identification makes it possible to study the information loss problem of an evaporating black hole through the study of the entanglement entropy between two universes in (2.3).

Since the universe B can be regarded as a bath collecting the Hawking quanta, it is often assumed that the universe B is non-gravitating. In this case, the entanglement entropy of the universe A is computed by the island formula (1.1). However, for an actual evaporating black hole in our universe, the Hawking quanta are always located in the gravitating region. This motivates us to study the setup where the universe B is also gravitating. This generalization is not only for the sake of precision. Instead, in this generalization, we expect a new physical effect, called ER=EPR [76] comes into play. This correspondence states that in a theory of gravity, two entangled systems must have a geometric connection through a wormhole. One

of the goals of this paper is to understand how ER=EPR affects the entropy of Hawking radiation.

We are interested in the entanglement entropy $S(\rho_A)$ of (2.3) on the universe A,

$$S(\rho_A) = -\operatorname{tr} \rho_A \, \log \rho_A, \quad \rho_A = \operatorname{tr}_B |\Psi\rangle\langle\Psi|. \tag{2.4}$$

In [54], this entropy $S(\rho_A)$ was computed through the replica trick, and the result reads,

$$S(\rho_A) = \operatorname{Min}\{S_{\text{th}}(\beta), \, S_{\text{swap}}(\rho_A)\}, \quad S_{\text{swap}}(\rho_A) = \min_{\overline{C}} \operatorname{ext} \left[\frac{\Phi_{A/B}(\partial\overline{C})}{4G_N} + S_{\beta/2}(\overline{C}) - S_{\text{vac}}(\overline{C}) \right]. \tag{2.5}$$

This expression is quite similar to a version of the island formula [28, 29, 49], which computes the same entropy of the same state (2.3) defined on a gravitating universe A and a *non*-gravitating universe B. However, there is one important difference between (2.5) and the island formula. Namely the dilaton profile $\Phi_{A/B}$ appears in (2.5) is neither the dilaton profile Φ_A on the universe A nor, Φ_B on the universe B.

Instead, $\Phi_{A/B}$ is the dilaton profile of a *new* spacetime A/B, which is constructed by gluing two universes A and B. For example, when A and B are both asymptotically AdS, the spacetime geometry of each universe Φ_A, Φ_B is specified by the boundary conditions at the left and right conformal boundaries (see figure 3). The dilaton profile on A/B has the boundary conditions for the universe A at its left conformal boundary, and the boundary conditions for B at its right boundary. One of the goals of this paper is to construct this glued geometry $\Phi_{A/B}$ for a variety of examples.

$S_{\beta/2}(\overline{C})$ in (2.5) denotes the entanglement entropy of the thermal ensemble of the bulk conformal field theory, with the inverse temperature $\beta/2$, and $S_{\text{vac}}(\overline{C})$ is the entanglement entropy of the vacuum.

We compute the generalized entropy $S_{\text{gen}}[\overline{C}] = \Phi_{A/B}(\partial\overline{C}) + S_{\beta/2}(\overline{C}) - S_{\text{vac}}(\overline{C})$ in the right hand side of (2.5) for all possible intervals $\overline{C}$ in A/B (see the right panel of figure 3), then extremize to obtain what we call the swap entropy $S_{\text{swap}}(\rho_A)$. The minimum between $S_{\text{swap}}(\rho_A)$ and the thermal entropy $S_{\text{th}}(\beta) \to 2\pi^2 c/3\beta, \beta \to 0$ gives the entanglement entropy $S(\rho_A)$ for the universe A. This rule for constructing $\Phi_{A/B}$ was obtained by properly including the wormhole saddle points of the corresponding Rényi entropy $\operatorname{tr} \rho_A^n$.
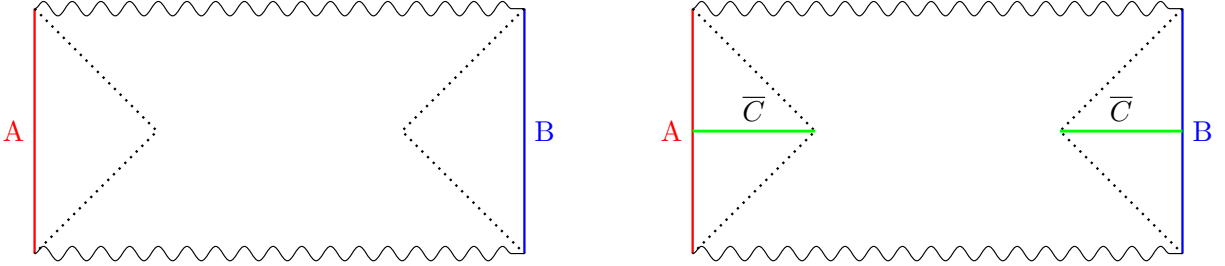
Figure 3: **Left**: The Penrose diagram of the new spacetime A/B in AdS. The spacetime is specified by the left and right conformal boundary conditions (red and blue vertical lines). **Right**: The same Penrose diagram of the new spacetime A/B with the region $\overline{C}$ (green region) on which we evaluate the generalized entropy $S_{\text{gen}}[\overline{C}]$.

Sketch of the derivation

For later convenience, let us sketch the derivation of the result (2.5) for AdS black holes [54]. To this end, we start from the replica trick for the entanglement entropy,

$$S(\rho_A) = \lim_{n \to 1} \frac{1}{1-n} \text{tr} \, \rho_A^n. \tag{2.6}$$

We then compute the right hand side for positive integers n. From the definition of the state (2.3), we have

$$\text{tr} \, \rho_A^n = \frac{1}{Z_1^n} \sum_{\{i_k, j_k\}=1}^{\infty} \prod_{k=1}^{n} \sqrt{p_{i_k} p_{j_k}} \, \langle \psi_{i_k} | \psi_{j_k} \rangle_{A_k} \, \langle \psi_{j_k} | \psi_{i_{k+1}} \rangle_{B_k}, \tag{2.7}$$

where $A_k(B_k)$ denotes the k-th copy of the universe A(B), with the normalization factor Z_1 defined by

$$Z_1 = \sum_{i,j=1}^{\infty} \sqrt{p_i p_j} \, \langle \psi_i | \psi_j \rangle_A \langle \psi_j | \psi_i \rangle_B. \tag{2.8}$$

The eternal black hole state in the universe A can be prepared by a Euclidean path integral on a half disc with an appropriate boundary condition at the conformal boundary. We collectively denote them by $\lambda_A(u)$, where u is the coordinate for the boundary circle. Similarly, we denote the boundary conditions for the black hole in B by $\lambda_B(u)$. Since each $|\psi_i\rangle_{A_k}$ is a small CFT excitation on top of the fixed black hole in A, we can prepare it again by a path integral on the half disc with $\lambda_A(u)$, but now with the insertion of a CFT operator corresponding to the excitation on the south pole of the half disc. Similarly each overlap $\langle \psi_{i_k} | \psi_{j_k} \rangle_{A_k}$ appearing in (2.7) is computed by inserting two local operators of the bulk CFT to the full disc. Altogether, the Rényi entropy (2.7) has a gravitational path integral

expression, with $2n$ circle boundaries $\{\partial A_k, \partial B_k\}$ with $4n$ CFT local operator insertions (see figure 4).
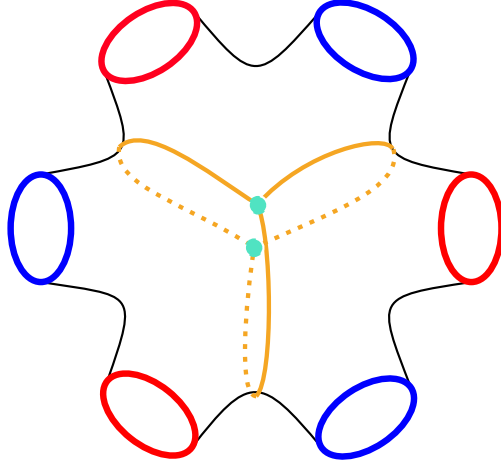
Figure 4: Schematic picture of the replica geometry M_{2n} ($n = 3$ case). The n ($n = 3$) red boundaries corresponds to the boundaries of the universe A, i.e., ∂A. The others (blue) correspond to the boundaries of the universe B, i.e., ∂B. The cyan dots are the fixed points of this replica geometry. Upon taking the quotient of the geometry by the replica symmetry $\mathbb{Z}_N$, the orange lines become the branch cuts.

As was shown in [54], in the high entanglement temperature limit $\beta \to 0$, the gravitational path integral is dominated by a single gravitational saddle M_{2n} where all the $2n$ boundaries $\{\partial A_k, \partial B_k\}$ are connected by a single wormhole. One way to think about this manifold is first introducing a wormhole connecting the disc A_k to the other B_k in the same replica to make them a cylinder (or equivalently an annulus), then connect these n cylinders by a replica wormhole. This manifold therefore has a replica symmetry $\mathbb{Z}_n$ which shifts the k-th replica to the $(k + 1)$-th.

The gravitational action of the saddle M_{2n} is computed by the standard trick developed in [77]. Since the saddle has a replica symmetry $\mathbb{Z}_n$, one can take its quotient $\tilde{M}_{2n} = M_{2n}/\mathbb{Z}_n$, which has the topology of an annulus with a cut, whose two boundary circles can be identified with the boundary of the universe A and B. Including the CFT operators, this path integral on the annulus can be written as the thermal correlator

$$\text{tr}\left[e^{-\beta_{\text{ann}}H/2}\psi_{i_k}\psi_{i_{k+1}}e^{-\beta_{\text{ann}}H/2}\psi_{j_k}\psi_{j_k}\right] \tag{2.9}$$

where β_{ann} denotes the circumference of the annulus, which should be distinguished from the entanglement temperature β (see figure 5). When the entanglement between A and B is strong $\beta \to 0$, it is natural to expect the renormalized length between two boundaries $\{\partial A_k, \partial B_k\}$

becomes shorter and shorter. This means that if we fix its spatial size, the circumference gets longer, $\beta_{\mathrm{ann}} \to \infty$. In this limit, one can replace $e^{-\beta_{\mathrm{ann}}H/2}$ to the projection operator $|0\rangle\langle 0|$, thus the annulus amplitude is split into two disc path integrals, one is with a cut, and the other without. See again figure 5. The path integral on the disc without the cut cancels with the path integral of Z_1 (2.8) in the denominator of (2.7). Finally, the $n \to 1$ limit the remaining path integral on the disc with the cut can be identified with the generalized entropy on the left hand side of (2.5). This manifests the origin of the appearance of $\Phi_{A/B}$ in (2.5). As is clear from figure 5 on the half boundary of this disk, we impose the boundary conditions of the universe A and on the other half we impose the condition for B.
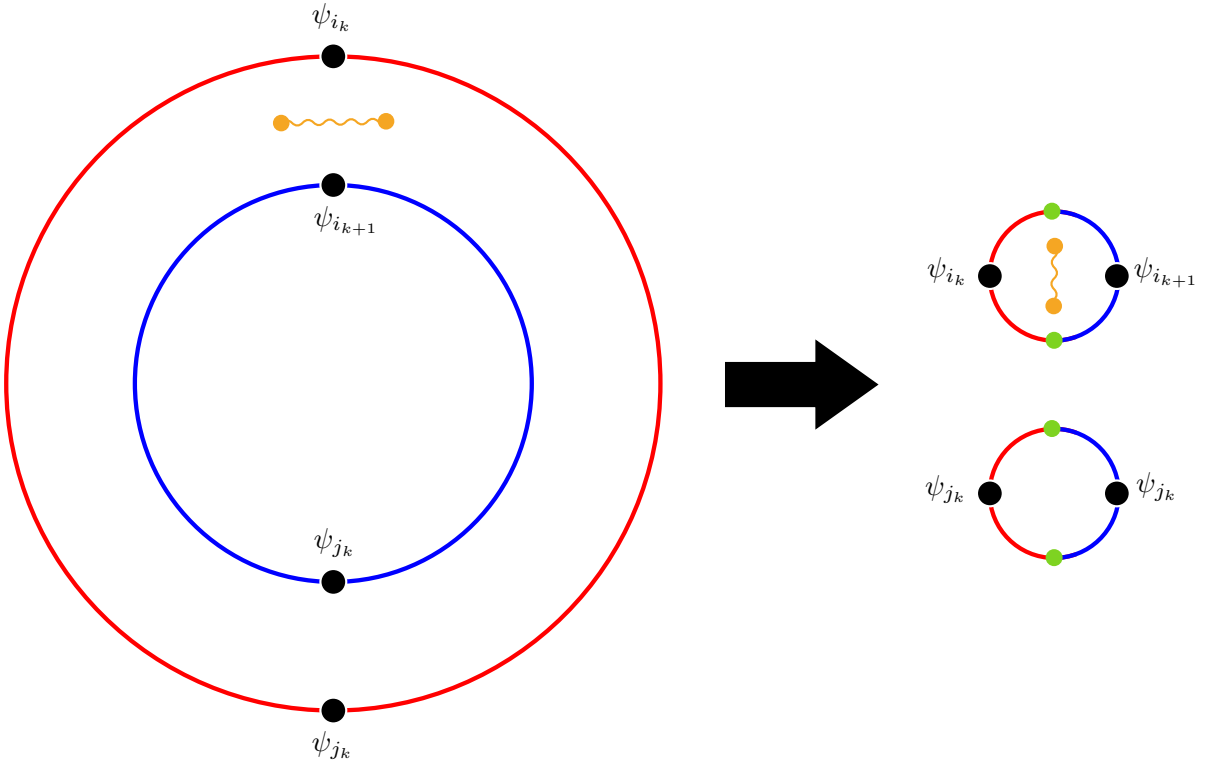
Figure 5: **Left**: Schematic picture of the annulus geometry $M_{2n}/\mathbb{Z}_n$. This annulus geometry has a cut (orange line) whose endpoints are the fixed points of the replica symmetry. **Right**: Schematic picture of the two disc geometries, which are obtained from the annulus geometry (left figure) by taking the $\beta \to 0$ limit. One of the two disks contains a cut (orange line). The green dots are boundary condition changing points between the two conditions of the universes A and B.

3 Entangled eternal black holes in AdS with two different masses

In this section, we discuss the construction of the glued geometry $\Phi_{A/B}$ which computes the entanglement entropy on two gravitating universes $(2.5)^2$. We focus on the case where the universe A is an eternal AdS black hole with the mass M_A, and similarly the universe B contains an AdS eternal black hole with M_B. We work in the global coordinates (μ, τ), where the AdS metric takes the following form,

$$ds^2 = \frac{-d\tau^2 + d\mu^2}{\cos^2 \mu}. \tag{3.1}$$

In the coordinates, the conformal boundaries are located at $\mu = \pm\frac{\pi}{2}$. The dilaton profile of the universe A is given by

$$\Phi_A(\mu, \tau) = b_A \frac{\cos \tau}{\cos \mu}, \tag{3.2}$$

where the parameter b_A is related to the black hole mass M_A through

$$M_A = \frac{b_A^2}{16\pi G \phi_b}. \tag{3.3}$$

We can see the above relation through the ADM mass formula (A.5). This dilaton profile represents an eternal black hole. We have a similar dilaton profile Φ_B for B.

The dilaton profile $\Phi_{A/B}$ which appears in the entropy functional (2.5) satisfies the following boundary conditions,

$$\Phi_{A/B} \to \Phi_A, \quad \mu \to \frac{\pi}{2}, \qquad \text{and} \qquad \Phi_{A/B} \to \Phi_B, \quad \mu \to -\frac{\pi}{2}, \tag{3.4}$$

thus $\Phi_{A/B}$ is the dilaton profile of a two sided black hole with different left and right masses. The dilaton profile satisfies the following equations of motion,

$$\frac{1}{\cos^2 \mu} \partial_+ \left[\cos^2 \mu \, \partial_+ \Phi \right] = -8\pi G \, \langle T_{++} \rangle_\beta,$$

$$\frac{1}{\cos^2 \mu} \partial_- \left[\cos^2 \mu \, \partial_- \Phi \right] = -8\pi G \, \langle T_{--} \rangle_\beta, \tag{3.5}$$

$$2\partial_+ \partial_- \Phi - \frac{1}{\cos^2 \mu} \Phi = 16\pi G \, \langle T_{+-} \rangle_\beta,$$

with the CFT stress energy tensor evaluated on the state (2.3)

$$\langle T_{++} \rangle_\beta = \langle T_{--} \rangle_\beta = \frac{c}{24\pi} \left(\frac{2\pi}{\beta} \right)^2 \equiv \langle T \rangle_\beta, \quad \langle T_{\pm\mp} \rangle_\beta = 0, \tag{3.6}$$

---

[2] See [78] for a related discussion.

where the chiral coordinates $x^{\pm}$ are defined by

$$x^{\pm} = \mu \pm \tau. \tag{3.7}$$

As we increase the entanglement temperature $1/\beta$, the eternal black hole (3.2) receives the back reaction from the CFT stress energy tensor $\langle T_{\pm\pm}\rangle_\beta$. The result reads [28],

$$\Phi_A(\mu,\tau) = \frac{b_A}{2}\left[\left(b_0 + \frac{1}{b_0}\right) - \frac{2}{\pi}\left(b_0 - \frac{1}{b_0}\right)(\mu\tan\mu + 1)\right], \tag{3.8}$$

where b_0 is related to $\langle T\rangle_\beta$ by

$$\frac{b_A}{\pi}\left(b_0 - \frac{1}{b_0}\right) = 16\pi G\langle T\rangle_\beta. \tag{3.9}$$

The mass M_A of the black hole remains unchanged by this back reaction.

Now let us specify the dilaton profile $\Phi_{A/B}$ which solves (3.5) and satisfies the boundary conditions (3.4). First, we note that the general solution of (3.5) is given by

$$\begin{aligned}\Phi(\mu,\tau) &= \Phi_0(\mu,\tau) - 16\pi G\langle T\rangle_\beta \ (\mu\tan\mu + 1)\\ &= \left(a\tan\mu + b\,\frac{\cos\tau}{\cos\mu}\right) - 16\pi G\langle T\rangle_\beta \ (\mu\tan\mu + 1),\end{aligned} \tag{3.10}$$

where Φ_0 denotes the "sourceless" part of the dilaton, satisfying (3.5) with the vanishing stress energy tensor $\langle T_{\mu\nu}\rangle = 0$, and this depends on two parameters a and b [3].

In the $\mu \to \frac{\pi}{2}$ limit, the solution (3.10) approaches

$$\Phi(\mu,\tau) = b\,\frac{\cos\tau}{\cos\mu} - \left(8\pi^2 G\langle T\rangle_\beta - a\right)\tan\mu. \tag{3.11}$$

This describes a black hole with the mass

$$M_R = \frac{1}{16\pi G\phi_b}\left(b^2 - \left(8\pi^2 G\langle T\rangle_\beta - a\right)^2\right). \tag{3.12}$$

This can be seen by directly using the ADM mass formula (A.5) or applying an $SL(2,\mathbb{R})$ transformation to the dilaton profile (3.11), which brings the event horizon to the center of the space $(\mu,\tau) = (0,0)$. Then the profile of the right Rindler wedge is that of the usual AdS Schwarzschild black hole.

---

[3] Although there is an additional term, $\frac{\sin\tau}{\cos\mu}$ for the general solution, we do not include such a term for simplicity. In the absence of this term, bifurcation surfaces are located on the $\tau = 0$ time slice, as explained later.

Similarly, by taking the $\mu \to -\frac{\pi}{2}$ limit of (3.10), we read off the mass of the left black hole,

$$M_L = \frac{1}{16\pi G\phi_b}\left(b^2 - \left(8\pi^2 G\langle T\rangle_\beta + a\right)^2\right) \tag{3.13}$$

We identify the left mass M_L to be the mass of the black hole in the universe A, $M_L = M_A$, and similarly $M_R = M_B$. These conditions fix the parameters a, b in the dilaton profile (3.10) to be

$$\begin{aligned} a &= \frac{\phi_b}{2\pi\langle T\rangle_\beta}\left(M_B - M_A\right) \\ b &= \sqrt{8\pi G\phi_b(M_A + M_B) + 64\pi^2 G^2\langle T\rangle_\beta^2 + \frac{\phi_b^2}{4\pi^2\langle T\rangle_\beta^2}\left(M_B - M_A\right)^2} \\ &\underset{\beta\to 0}{\approx} \sqrt{8\pi G\phi_b(M_A + M_B) + 64\pi^2 G^2\langle T\rangle_\beta^2}. \end{aligned} \tag{3.14}$$

3.1 The Penrose digram of the glued geometry in JT gravity

Having specified the dilaton profile $\Phi_{A/B}$ of the glued spacetime A/B, now let us study the causal structure of the black hole. We are particularly interested in the high entanglement temperature limit $\beta \to 0$.

Let us first specify the locations of the bifurcation surfaces. These surfaces extremizes the profile $\partial_\tau \Phi_{A/B} = \partial_\mu \Phi_{A/B} = 0$. It turns out that there are two such surfaces at $\mu = \mu_R$, μ_L on the time slice $\tau = 0$. First, let us consider the right horizon, at $\mu = \mu_R, \tau = 0$. As we will see, this horizon approaches the right boundary $\mu_R \to \frac{\pi}{2}$ in the limit of our interest $\beta \to 0$, so near the right horizon we can approximate the dilaton profile as (3.11), with the parameters (3.14). Then we get

$$\sin\mu_R = \frac{1}{b}\left(8\pi^2 G\langle T\rangle_\beta - a\right). \tag{3.15}$$

In this limit, the value of the dilaton profile at this surface is

$$\Phi_{A/B}(\mu = \mu_R, \tau = 0) \to b_A, \quad \beta \to 0, \tag{3.16}$$

where b_A is defined in (3.3). This is expected, since $\Phi_{A/B} \to \Phi_A$ near the right conformal boundary. Similarly in the high entanglement temperature limit $\beta \to 0$, the left horizon approaches the left boundary $\mu_L \to -\frac{\pi}{2}$, and satisfies,

$$\sin\mu_L = \frac{1}{b}\left(8\pi^2 G\langle T\rangle_\beta + a\right). \tag{3.17}$$

thus the dilaton value at the horizon is $\Phi(\mu_L, 0) = b_B$.

Since these two horizons move toward different conformal boundaries $\mu_R \to \frac{\pi}{2}$ and $\mu_L \to -\frac{\pi}{2}$ as we decrease β, the black hole develops a large interior region between the two horizons. Since this is inaccessible from both left and right conformal boundaries, it is often called a causal shadow region. Finally the singularity of the black hole is located at $\Phi_{A/B}(\mu, \tau) = 0$. Taking into account these, we get the Penrose diagram (figure 6) for the glued geometry A/B with the dilaton profile $\Phi_{A/B}$ in JT gravity. A similar dilaton profile was discussed for example in [28].
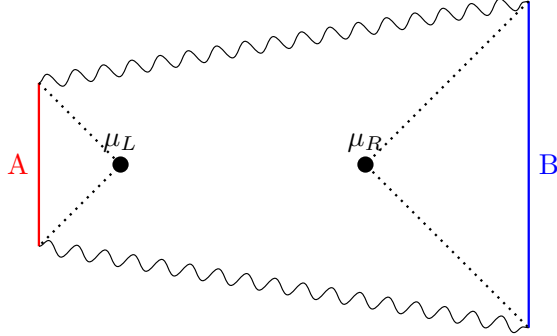
Figure 6: The Penrose diagram of the glued spacetime A/B with two distinct black hole masses $M_A \neq M_B$ in JT gravity.

4 Entangled eternal black holes in flat space with two different masses

In this section, we construct the dilaton profile $\Phi_{A/B}$ in CGHS gravity, starting from two asymptotically flat black holes in A and B with distinct masses M_A, M_B. We begin our discussion from the following expression of the flat space metric,

$$ds^2 = \frac{dx^+ dx^-}{\cos^2 x^+ \cos^2 x^-}, \tag{4.1}$$

related to the standard form $ds^2 = dX^+ dX^-$ by the coordinate transformation $X^\pm = \tan x^\pm$. The asymptotic spatial infinity is located at $x^+ = \pm\frac{\pi}{2}$ or $x^- = \pm\frac{\pi}{2}$. The equations of motion of CGHS gravity are given by

$$-\frac{1}{\cos^2 x^+}\partial_+ \left[\cos^2 x^+ \partial_+\right] \Phi = 8\pi G \left\langle T_{++}\right\rangle_\beta,$$
$$-\frac{1}{\cos^2 x^-}\partial_- \left[\cos^2 x^- \partial_-\right] \Phi = 8\pi G \left\langle T_{--}\right\rangle_\beta, \tag{4.2}$$
$$2\partial_+\partial_-\Phi = 16\pi G \left\langle T_{+-}\right\rangle_\beta - \frac{\Lambda}{2}\frac{1}{\cos^2 x^+ \cos^2 x^-},$$

where the expectation value of the stress energy tensor $\langle T_{\mu\nu}\rangle_\beta$ is again given by (3.6).

When there is no entanglement in the state (2.3), i.e., $\beta = \infty$, the dilaton profile for the eternal black hole in A is

$$\Phi_A^0 = \phi_{0,A} + \frac{|\Lambda|}{4} \tan x^+ \tan x^-. \tag{4.3}$$

The mass of this black hole is given by

$$M_A = \frac{\sqrt{|\Lambda|}}{16\pi G} \phi_{0,A}, \tag{4.4}$$

where we used the ADM formula (A.8). A similar profile for the black hole in the universe B is obtained by the replacement $\phi_{0,A} \to \phi_{0,B}$ in (4.3). This black hole has the unique bifurcation surface at $x^\pm = 0$.

As we increase the entanglement temperature $1/\beta$, these black holes receive back reaction from the CFT stress energy tensor. From the equations of motion (4.2), we find the dilaton profile with the back reaction is [49]

$$\Phi_A(x^+, x^-) = \phi_{0,A} + \frac{|\Lambda|}{4} \tan x^+ \tan x^- - 4\pi G \langle T \rangle_\beta \left(x^+ \tan x^+ + x^- \tan x^-\right), \tag{4.5}$$

where $\langle T \rangle_\beta \equiv \langle T_{\pm\pm} \rangle_\beta$ is given by (3.6). Again we have a similar expression for the universe B. The mass of this black hole is given by

$$M_A = \frac{\sqrt{|\Lambda|}}{16\pi G} \left(\phi_{0,A} - \frac{\left(4\pi^2 G \langle T \rangle_\beta\right)^2}{|\Lambda|}\right). \tag{4.6}$$

M_A decreases as we increase the entanglement temperature $1/\beta$. This is in contrast with the similar black hole in AdS JT gravity (3.8) whose mass kept fixed under the increase.

Having specified the dilaton profiles Φ_A and Φ_B, let us construct $\Phi_{A/B}$ in CGHS model. The boundary conditions for $\Phi_{A/B}$ are given by

$$\Phi_{A/B} \to \Phi_A, \quad x^\pm \to -\frac{\pi}{2}, \qquad \text{and} \qquad \Phi_{A/B} \to \Phi_B, \quad x^\pm \to \frac{\pi}{2}. \tag{4.7}$$

This condition is analogous to the one in JT gravity (3.4). The general solution for (4.2) is given by

$$\begin{aligned}
\Phi_{A/B}(x^+, x^-) &= \Phi_0(x^+, x^-) - 4\pi G \langle T \rangle_\beta \left(x^+ \tan x^+ + x^- \tan x^-\right) \\
&= \left(D^0 + \frac{|\Lambda|}{4} \tan x^+ \tan x^- + D^+ \tan x^+ + D^- \tan x^-\right) \\
&\quad - 4\pi G \langle T \rangle_\beta \left(x^+ \tan x^+ + x^- \tan x^-\right)
\end{aligned} \tag{4.8}$$

where Φ_0 is the "sourceless" part , which satisfies the equations of motion with $\langle T_{\mu\nu} \rangle = 0$. The parameters $D^{0,\pm}$ in Φ_0 are determined from the conditions (4.7). We are mainly interested

in $D^+ = D^- \equiv D$ cases, which correspond to the situations where two bifurcation surfaces of the black hole are located on the $t = 0$ time slice[4]. To determine these parameters D^0, D, we focus on the asymptotic behaviors at $x^\pm \to \frac{\pi}{2}$ and $x^\pm \to -\frac{\pi}{2}$. In the right asymptotic limit $x^\pm \to \frac{\pi}{2}$, the dilaton profile $\Phi_{A/B}$ takes the form

$$\Phi_{A/B} \to \Phi_R = D^0 + \frac{|\Lambda|}{4} \tan x^+ \tan x^- + \left(D - \frac{\pi}{2} \cdot 4\pi G \langle T \rangle_\beta \right) (\tan x^+ + \tan x^-) \quad \text{as } x^\pm \to \frac{\pi}{2}, \tag{4.9}$$

where we introduced the notation Φ_R to distinguish it from the original one (4.5).

By using the ADM black hole mass formula (A.8), we can see that this dilaton profile Φ_R corresponds to a black hole with the mass

$$M_R = \frac{\sqrt{|\Lambda|}}{16\pi G} \left(D^0 - \frac{4}{|\Lambda|} \left(D - 2\pi^2 G \langle T \rangle_\beta \right)^2 \right). \tag{4.10}$$

On the other hand, in the left asymptotic limit $x^\pm \to -\frac{\pi}{2}$, the dilaton profile $\Phi_{A/B}$ becomes

$$\Phi_{A/B} \to \Phi_L = D^0 + \frac{|\Lambda|}{4} \tan x^+ \tan x^- + \left(D + \frac{\pi}{2} \cdot 4\pi G \langle T \rangle_\beta \right) (\tan x^+ + \tan x^-) \quad \text{as } x^\pm \to -\frac{\pi}{2}, \tag{4.11}$$

where we again introduced the notation Φ_L, and from the ADM mass formula (A.8) this dilaton profile Φ_L gives the black hole mass

$$M_L = \frac{\sqrt{|\Lambda|}}{16\pi G} \left(D^0 - \frac{4}{|\Lambda|} \left(D + 2\pi^2 G \langle T \rangle_\beta \right)^2 \right). \tag{4.12}$$

We identify these black hole masses M_L, M_R with M_A defined in (4.6) and M_B obtained by the replacement $\phi_{0,A} \to \phi_{0,B}$ in M_A respectively, i.e, $M_L = M_A$ and $M_R = M_B$. These identifications determine the parameters D^0, D in terms of $\phi_{0,A}$, $\phi_{0,B}$ and $\langle T \rangle_\beta$ as follows

$$\begin{aligned} D^0 &= \frac{\phi_{0,A} + \phi_{0,B}}{2} + |\Lambda| \frac{(\phi_{0,A} - \phi_{0,B})^2}{256\pi^4 G^2 \langle T \rangle_\beta^2} \\ &\underset{\beta \to 0}{\approx} \frac{\phi_{0,A} + \phi_{0,B}}{2}, \\ D &= |\Lambda| \frac{\phi_{0,B} - \phi_{0,A}}{32\pi^2 G \langle T \rangle_\beta}. \end{aligned} \tag{4.13}$$

4.1 The Penrose diagram in the CGHS gravity

Let us study the causal structure of the dilaton profile $\Phi_{A/B}$ obtained by plugging (4.13) into (4.8) in CGHS model. We are again interested in the high entanglement temperature limit $\beta \to 0$.

---

[4]The coordinates $x^\pm$ are related to t by $x^\pm = x \pm t$.

At first, we determine the locations of the bifurcation surfaces of the black hole, at which the dilaton profile $\Phi_{A/B}$ takes extremal values. From the extremality conditions $\partial_\pm \Phi_{A/B} = 0$, we get two distinct extremal surfaces $x_R^+ = x_R^- \equiv x_R$, $x_L^+ = x_L^- \equiv x_L$, which are located on the $t = 0$ time slice.

In the limit $\beta \to 0$, the extremality conditions take the following simple form

$$\tan x_R = -\frac{4}{|\Lambda|} \left(D - 2\pi^2 G\langle T\rangle_\beta \right), \quad \tan x_L = -\frac{4}{|\Lambda|} \left(D + 2\pi^2 G\langle T\rangle_\beta \right). \tag{4.14}$$

These equations imply that, in the limit $\beta \to 0$, the right bifurcation surface approaches the right spatial infinity $x_R^\pm \to \frac{\pi}{2}$ and the left one does the left spatial infinity $x_L^\pm \to -\frac{\pi}{2}$.

In this limit, the dilaton values at the bifurcation surfaces are given by

$$\begin{aligned}
\Phi_{A/B}(x^\pm = x_R) &\to D^0 - \frac{4}{|\Lambda|}\left(D - 2\pi^2 G\langle T\rangle_\beta\right)^2 = \phi_{0,B} - \frac{\left(4\pi^2 G\langle T\rangle_\beta\right)^2}{|\Lambda|}, \\
\Phi_{A/B}(x^\pm = x_L) &\to D^0 - \frac{4}{|\Lambda|}\left(D + 2\pi^2 G\langle T\rangle_\beta\right)^2 = \phi_{0,A} - \frac{\left(4\pi^2 G\langle T\rangle_\beta\right)^2}{|\Lambda|}.
\end{aligned} \qquad \text{as } \beta \to 0. \tag{4.15}$$

These dilaton values at the horizons are also consistent with the discussion in the previous section. From the above discussion plus the location of the singularity at $\Phi_{A/B}(x^+, x^-) = 0$, we get the Penrose diagram (figure 7) corresponding to the dilaton profile $\Phi_{A/B}$ in the CGHS gravity.
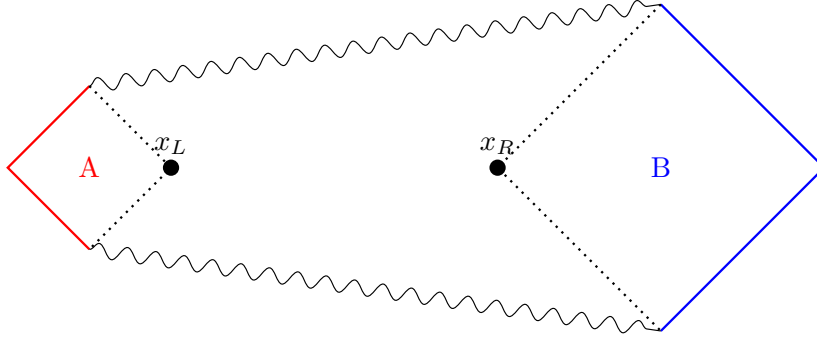
Figure 7: The Penrose diagram of the glued spacetime A/B with two different black hole masses in CGHS gravity.

5   Entropy calculation and its interpretation

In this section, we compute the entanglement entropy $S(\rho_A)$ using (2.5), by plugging the dilaton profile $\Phi_{A/B}$ of the glued geometry into the formula. We take the following ansatz

for $\bar{C}$ on the reflection symmetric slice,

$$\bar{C}: \left[-\frac{\pi}{2} - \frac{\pi y}{2}\right] \cup \left[\frac{\pi x}{2}, \frac{\pi}{2}\right], \quad 0 < x, y < 1, \tag{5.1}$$

see figure 3 for the AdS case.

Let us assume the bulk CFT has a holographic dual. Then the bulk entanglement entropies have the following simple expressions

$$S_{\beta/2}[\bar{C}] = \frac{c}{3} \log \left[\frac{\beta}{2\pi} \sinh \frac{\pi^2}{\beta} \left(1 - \frac{x+y}{2}\right)\right], \quad S_{\text{vac}}[\bar{C}] = \frac{c}{3} \log \left[2 \sin \pi \left(\frac{x+y}{2}\right)\right]. \tag{5.2}$$

The actual dilaton profile is given by (3.10) with (3.14) for AdS JT gravity, and (4.8) with (4.13) for flat CGHS model. Then $S_{\text{swap}}(\rho_A)$ in (2.5) is computed by taking the extrema of the following function with respect to two variables x and y,

$$S_{\text{gen}}(x,y) = \frac{\Phi_{A/B}(x)}{4G_N} + \frac{\Phi_{A/B}(y)}{4G_N} + \frac{c}{3} \log \left[\frac{\beta}{2\pi} \sinh \frac{\pi^2}{\beta} \left(1 - \frac{x+y}{2}\right)\right] - \frac{c}{3} \log \left[2 \sin \pi \left(\frac{x+y}{2}\right)\right]. \tag{5.3}$$

In both cases, in the $\beta \to 0$ limit, the bifurcation surfaces approach the asymptotic boundaries (or spatial infinities). The value of the entropy is half of the sum of the entropies of the original black holes,

$$S_{\text{swap}}(\rho_A) = S_{BH_A} + S_{BH_B} \tag{5.4}$$
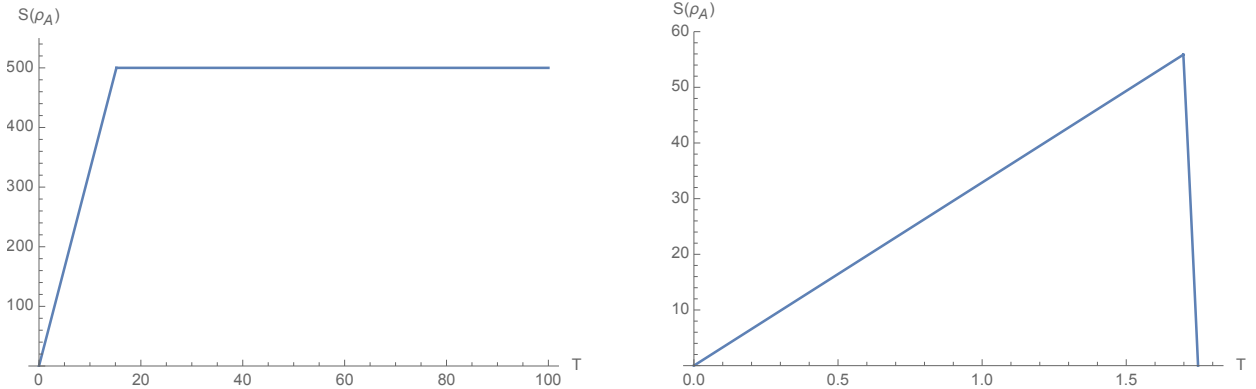
Figure 8: **Left**: Plots of the entanglement entropy (2.5) of the AdS JT gravity case as a function of the entanglement temperature $T = 1/\beta$. We set the parameters to be $\phi_{0,A} = 300$, $\phi_{0,B} = 200$, $c = 10$, $4G_N = 1$. **Right**: Similar Plots for flat CGHS model case as a function of $T = 1/\beta$. We set the parameters to be $\phi_{0,A} = 300$, $\phi_{0,B} = 200$, $|\Lambda| = 100$, $c = 10$, $4G_N = 1$.

We plot the resulting entanglement entropy (2.5) as a function of the entanglement temperature $1/\beta$ in figure 8 for black holes in AdS JT gravity as well as in flat CGHS model. In both cases, in the low temperature limit the results coincide with the thermal entropy of the bulk CFT, which reproduce the Hawking's result. In the high temperature regime where the results are proportional to the area of the black holes, two cases show distinct behaviors. Namely, whereas for the black holes in AdS JT gravity, the entanglement entropy saturates to a constant value, for the black holes in flat CGHS model, the entropy is decreasing. This difference can be understood from the fact that the black holes in flat space can evaporate by emitting Hawking quanta and lose their masses, on the contrary to the black holes in AdS.

We emphasize that our result is not obtained by applying the island formula for the universe A and B independently, then summing up their outcomes. Such a contribution would come from the replica wormhole connecting n copies of A and the other replica wormhole connecting Bs, without any further connection between A and B. However, as was argued in [54] this does not yield the expected result, i.e., the sum of two island formulae for A and B. This is because , in this saddle, the bulk CFT part of the path integral can not be interpreted as a Rényi entropy, due to the alignment of the operators the numerator of (2.7). Also, if we choose this saddle, then one can not kill the unbounded growth of the denominator. Thus the resulting entropy increases without any bound as well, in the high temperature limit.

6 Approximate gluings

We have discussed exact solutions for $\Phi_{A/B}$ for the asymptotically AdS black holes (3.2) and those in flat space (4.5). This was possible because the original dilaton profiles in A and B are simple enough to find such interpolating solutions $\Phi_{A/B}$. Then the question arises, is there any way to approximately construct such an interpolating solution, especially when it is difficult to find an exact solution. In this section we propose an idea in this direction, using shock waves in these geometries. Again, let us take the AdS black hole with the mass M_A (3.2) and the one with M_B for example, and think gluing them to obtain $\Phi_{A/B}$ by an approximate mean. We start from the dilaton profile (3.2), and then imagine inserting a left moving shock wave in the black hole interior. The expectation value of the CFT stress energy tensor is given by

$$\langle T_{\pm\pm} \rangle = \langle T_{\pm\pm} \rangle_\beta + \langle T_{\pm\pm} \rangle_S, \quad \langle T_{\pm\mp} \rangle = 0, \tag{6.1}$$

with

$$\langle T_{++} \rangle_S = E\delta(x^+ - x_0^+), \quad \langle T_{--} \rangle_S = 0. \tag{6.2}$$

Here we also added the thermal expectation value $\langle T_{\pm\pm} \rangle_\beta$ coming from the entanglement temperature. Now the set of equations of motion for the dilaton is given by (3.5) with the

above stress tensor (6.1). The new geometry depends on two parameters, the energy E of the shock wave, and its location $x^+ = x_0^+$. As we show in appendix B, the mass of the black hole to the right of the shock is changed to $M_{AR} = M_{AR}(x_0^+, E)$ from its original mass M_A. On the other hand, the mass of the left black hole remains to be the same, $M_{AL} = M_A$. The explicit form of the dilaton profile reads,

$$\Phi = b_A \left(\frac{\cos\tau}{\cos\mu} \right) - 16\pi G \langle T \rangle_\beta (\mu \tan\mu + 1)$$

$$- 16\pi G E \cos^2 \left(\frac{x_0^+ + x^-}{2} \right) \left[\tan\mu - \tan \left(\frac{x_0^+ + x^-}{2} \right) \right] \Theta(x^+ - x_0^+). \qquad (6.3)$$

To approximate the glued geometry $\Phi_{A/B}$ by the dilaton profile with the shock (6.3), we impose the condition that the right mass coincides with the mass of the black hole in B, $M_{AR}(x_0^+, E) = M_B$. Let us denote the dilaton profile (6.3) with this condition by $\tilde{\Phi}_{A/B}$. Details of the expression of $M_{AR}(x_0^+, E)$ can be found in Appendix B. Of course, this is not enough to entirely fix these two parameters x_0^+, E. However as we can immediately see, if we plug the approximate dilaton profile $\tilde{\Phi}_{A/B}$ into the generalized entropy (2.5) then extremize, then it gives the correct swap entropy $S_{\text{swap}}(\rho_A)$ in the $\beta \to 0$ limit, as long as the constraint is satisfied, because the resulting entropy is again given by the sum of two entropies of the black holes in A and B. We can also see, the only the difference between the true dilaton profile $\Phi_{A/B}$ and the approximate one $\tilde{\Phi}_{A/B}$ the presence of the term proportional to $\sin\tau / \cos\mu$, which only shifts the location of the horizon in the timelike direction.

We have a similar construction for CGHS model, and explain it in appendix C.

7 More general settings

So far, we have been discussing the cases where two horizons of the eternal black hole of each universe have the same masses $M_L = M_R$. When they are different, we should carefully construct the glued spacetime A/B on which we compute the generalized entropy.

As an example of such eternal black holes with $M_L \neq M_R$, let us again consider the dilaton profile of the form (3.10), which we reproduce here,

$$\Phi_A(\mu, \tau) = \left(a_A \tan\mu + b_A \frac{\cos\tau}{\cos\mu} \right) - 16\pi G X (\mu \tan\mu + 1). \qquad (7.1)$$

In previous sections, we regard this as the dilaton profile of the glued geometry A/B, which results from gluing two eternal black holes with the $M_{AL} = M_{AR}$, and $M_{BL} = M_{BR}$,

but now we regard it as an example of the dilaton profile of the single universe, say the universe A, with $M_{AL} \neq M_{AR}$. Also in this setup, we are regarding the parameter X as merely a parameter, not related to the entanglement temperature $1/\beta$ and the corresponding CFT stress tensor $\langle T \rangle_\beta$.

The masses of the left and right black holes M_{AL}, M_{AR} are given by

$$M_{AL} = \frac{1}{16\pi G \phi_b} \left(b_A^2 - \left(8\pi^2 G X + a_A \right)^2 \right), \quad M_{AR} = \frac{1}{16\pi G \phi_b} \left(b_A^2 - \left(8\pi^2 G X - a_A \right)^2 \right). \tag{7.2}$$

We also have a similar dilaton profile for the universe B by the replacement $(a_A, b_A) \to (a_B, b_B)$ in (7.1), while keeping X intact.

Now we would like to specify the dilaton profile of the glued geometry $\Phi_{A/B}$ which appears in the formula for the entanglement entropy (2.5). In this generalized case, there are four candidates of the dilaton profile, namely $\Phi_{AL/BR}$, $\Phi_{AL/BL}$, $\Phi_{AR/BL}$, $\Phi_{AR/BR}$. Here for example we denote by $\Phi_{AL/BR}$ the dilaton profile which approaches Φ_A near the left boundary and Φ_B near the right boundary, satisfies the following boundary conditions,

$$\Phi_{A/B} \to \Phi_A, \quad \mu \to -\frac{\pi}{2}, \qquad \text{and} \qquad \Phi_{A/B} \to \Phi_B, \quad \mu \to +\frac{\pi}{2}. \tag{7.3}$$

This dilaton profile $\Phi_{AL/BR}$ contains the left horizon of the black hole in A and the right horizon of the black hole in B. Other dilaton profiles are also defined in a similar way, according to the choice of two horizons in A/B out of candidate horizons $\{AL, AR\}$ in A and $\{BL, BR\}$ in B. They all satisfy the equations of motion (3.5) with $\langle T_{++} \rangle = \langle T_{--} \rangle = \langle T \rangle_\beta + X$. The difference between them is coming from the choice of the boundary conditions near the conformal boundaries $\mu \to \pm\frac{\pi}{2}$.

One may be puzzled by the fact that we are dealing with dilaton profiles obeying distinct boundary conditions, for the reason that in a calculation of a semi-classical gravitational path integral we always fix the boundary conditions. To clarify this point, let us come back to the replica derivation of the formula (2.5) which was briefly reviewed in section 2, as in figure 4. The entanglement entropy is computed by evaluating the on shell action of the Euclidean wormhole connecting two discs for the universes A and B, in the presence of a cut $\overline{C}$. In this description we have a unique boundary condition on ∂A and ∂B. When the masses of the left and right horizons are not necessarily the same $M_{AL} \neq M_{AR}, M_{AL} \neq M_{AR}$, there are four possible types of Euclidean wormholes. Such a wormhole is constructed first by flipping the left and right of these discs, then connecting these two. For example, suppose that we flip the disc of the universe B and then connect A and B. Its Lorenzian continuation of the Euclidean cylinder gives two eternal black holes, one of which contains the cut $\overline{C}$.

Furthermore, as is explained in [54] these two eternal black holes gets disjoint in the high entanglement temperature limit $\beta \to 0$, as depicted in figure 5. This is because if we regard the cylinder as an annulus, its circumference gets large in this limit. Therefore, for the eternal black hole with the cut, when analytically continued, the dilaton is given by $\Phi_{AR,BR}$[5]. Similarly, if we flip both two universes we get a wormhole whose Lorenzian dilaton profile is given by $\Phi_{AL,BR}$.

For each wormhole with the cut $\overline{C}$, the gravitational action is proportional to its dilaton profile $-(n-1)\Phi[\overline{C}]$ in the $n \to 1$ limit. Upon taking the extremization, this picks up the extremal surface $\partial_{\partial\overline{C}}\Phi_{A/B} = 0$, on which the dilaton value is equal to the area of the horizon of the relevant black hole. The dominant saddle of the gravitational path integral can be found by taking the minimum value among these four candidates $\{\Phi_{AL/BR}, \ \Phi_{AL/BL}, \ \Phi_{AR/BL}, \Phi_{AR/BR}\}$. On the other hand the value of the denominator is independent from the choice of the wormhole, i.e., in the absence of the cut, their action values are always the same.

By combining these, we conclude that in the high temperature limit $\beta \to 0$, the entanglement entropy is given by the sum of the two smallest black hole entropies. In our case, it is given by

$$S(\rho_A) = \text{Min}[S_{AL} + S_{BL}, \ S_{AL} + S_{BR}, \ S_{AR} + S_{BR}, \ S_{AR} + S_{BL}]. \tag{7.4}$$

We can also construct dilaton profiles describing general glued geometries in CGHS model too. This construction is parallel to the one in the previous sections 4. In this case, we consider the following dilaton profile

$$\Phi_A(x^+, x^-) = \phi_{0,A} + \frac{|\Lambda|}{4} \tan x^+ \tan x^- - 4\pi G X \left(x^+ \tan x^+ + x^- \tan x^- \right)$$
$$+ D_A(\tan x^+ + \tan x^-) \tag{7.5}$$

for the universe A, and similarly for the universe B. This dilaton profile Φ_A corresponds to a black hole with the masses

$$M_{AR} = \frac{\sqrt{|\Lambda|}}{16\pi G} \left(\phi_{0,A} - \frac{4}{|\Lambda|} \left(D_A - 2\pi^2 G X \right)^2 \right), \quad M_{AL} = \frac{\sqrt{|\Lambda|}}{16\pi G} \left(\phi_{0,A} - \frac{4}{|\Lambda|} \left(D_A + 2\pi^2 G X \right)^2 \right), \tag{7.6}$$

and similarly for Φ_B.

For these masses, by repeating the analysis of the section 4, we get various dilaton profiles $\Phi_{AL/BR}, \ \Phi_{AL/BR}, \ \Phi_{AR/BL}, \Phi_{AR/BL}$ as in the case of JT gravity. Namely, each

---

[5]Notice that without any flip, we get the dilaton $\Phi_{AR,BL}$, because as in [54] we rotate the disc B by π relative to the disc A, to adjust the locations of the CFT operators.

dilaton profile can be constructed starting from the general solution (4.8) with the replacement $\langle T \rangle_\beta \to \langle T \rangle_\beta + X$ with the boundary conditions analgous to (4.7).

8 Conclusion and discussions

In this paper, we consider the entanglement entropy of states defined on two disjoint universes, by generalizing the argument of [54].

Let us interpret the result we obtained. We started from the entangled state (2.3) on two disjoint gravitating universes A and B. Since there is a black hole on the universe B, this state can be regarded as an entangled state of the Hawking quanta in the universe A and black hole microstates in the universe B. This interpretation is similar to the setup for the island formula, where one takes the bath universe to be non gravitating. In the latter case, although the number of the degrees of freedom in the non-gravitating universe is infinite, the maximal entanglement that the system can accommodate is given by the entropy of the black hole in the universe B in accord with the structure of the total Hilbert space.

In the current setup where both of these universes are gravitating, this scenario gets modified. Namely, as is clear from the formula (2.5), the gravitational dynamics completely changes the system. After the dominant saddle in (2.5) is changed, it becomes a system where the Hawking radiation is entangled with the black holes in A/B, whose detailed properties were studied in this paper. Thus we speculate the interior region of the new black hole belongs to the entanglement wedge of the Hawking radiation. Such a gluing happens due to the back reaction of the stress tensor induced from the entanglement between two universes, A and B. This can be regarded as a concrete realization of ER=EPR [76], which relates entanglement in presence of gravity to spatial wormholes.

It would be interesting to study this phenomenon further, with emphasis on its microscopic origin. One consistent description of an evaporating black hole is in terms of a class of states of the form

$$|\Psi\rangle = \sum_{\alpha,i} C_{\alpha,i} |\psi_\alpha\rangle_{BH} \otimes |i\rangle_R \tag{8.1}$$

where $C_{\alpha,i}$ is a random matrix drawn from Gaussian ensemble, and $|\psi_\alpha\rangle_{BH}$, $|i\rangle_R$ are orthonomal basis of the Hilbert space of black hole microstates H_{BH}, and the similar basis for Hawking radiation H_R respectively. This point of view of evaporating black holes was first studied by Page [3]. The randomness of the coefficient matrix is coming from the chaotic nature of the black hole dynamics. Averaging over these random matrices leads to a semiclassical description, but consistent with the principles of quantum theory. For example the

Page curve of the radiation entropy as well as the island formula follows from it. From this point of view, the island region in the black hole interior can be regarded as a region accommodating random fluctuations in the entangled state (8.1). See [79] for a recent discussion on this topic and its relation to baby universes. Since the system we studied in this paper involves two such black holes, it is natural to expect that the microscopic description of the setup has to do with two such random matrices. Related discussions toward this direction can be found in [48, 80].

Acknowledgement

A   ADM Mass formula

In this appendix, we give ADM mass formulae in AdS JT gravity and CGHS gravity. We also give the explicit ADM masses of general dilaton profiles in both cases.

A.1   ADM mass formula in AdS JT gravity

We consider the ADM mass of a dilaton profile in AdS JT gravity. The relation between dilaton profiles and the ADM black hole mass is discussed in e.g. [81, 82]. To introduce the ADM mass formula, we need to specify boundary conditions of the metric and the dilaton on the asymptotic boundary. We assume that they are given by

$$\Phi|_{bdy} = \frac{\phi_b}{\varepsilon}, \tag{A.1}$$

$$g_{uu}|_{bdy} = -\frac{1}{\varepsilon^2}, \tag{A.2}$$

where ε is the cutoff, ϕ_b is the renormalized dilaton value, which is a constant at the cutoff surface, and u is a boundary time coordinate along the cutoff surface. Also $|_{bdy}$ implies that we evaluate the expression at the boundary.

Then the ADM mass formula associated with one side of the two AdS boundaries is given by

$$M_{ADM} = -\frac{\sqrt{-g_{uu}}}{8\pi G}(\partial_n \Phi - \Phi)|_{bdy}, \tag{A.3}$$

where n is the (outward) normal vector to the boundary, ∂_n denotes the normal derivative to the boundary.

For example, we consider a dilaton profile Φ satisfying the equations of motion (3.10) with vanishing stress energy tensor. The general solution is given by

$$\Phi = Q_{-1}\frac{\cos\tau}{\cos\mu} + Q_0\frac{\sin\tau}{\cos\mu} - Q_1\tan\mu, \tag{A.4}$$

where Q_{-1}, Q_0, Q_1 are constants.

For this general dilaton profile, the ADM black hole mass associated with one side of the AdS boundaries becomes

$$M_{ADM} = \frac{(Q_{-1})^2 + (Q_0)^2 - (Q_1)^2}{16\pi G\phi_b}. \tag{A.5}$$

This expression is manifestly invariant under the $SL(2,\mathbb{R})$ rotation, which is a symmetry of JT gravity.

A.2 ADM mass formula in Flat CGHS gravity

Next we consider the ADM black hole mass described by a dilaton profile in CGHS gravity. For CGHS gravity, the relation between dilaton profiles and the ADM black hole mass is discussed in e.g. [83, 84].

The ADM mass formula associated with one side of the two spatial infinities is given by

$$M_{ADM} = \frac{1}{16\pi G\sqrt{|\Lambda|}} \left(-(\nabla\Phi)^2 + |\Lambda|\Phi\right)|_{\text{sp.inf.}}, \tag{A.6}$$

where $|_{\text{sp.inf.}}$ implies that we evaluate the expression at a spatial infinity.

As in the case of JT gravity, we consider a dilaton profile Φ satisfying the equations of motion (4.2) with vanishing stress energy tensor. The general solution is given by

$$\Phi = D^0 + \frac{|\Lambda|}{4}\tan x^+ \tan x^- + D^+ \tan x^+ + D^- \tan x^-, \tag{A.7}$$

where $D^{0,\pm}$ are constants.

This dilaton profile gives the ADM black hole mass associated with one side of the two spatial infinities

$$M_{ADM} = \frac{\sqrt{|\Lambda|}}{16\pi G}\left(D^0 - \frac{4}{\sqrt{|\Lambda|}}D^+D^-\right). \tag{A.8}$$

B   The black hole solution with a shockwave in its interior (AdS JT gravity)

In this appendix, we explain a method to construct a dilaton profile describing a glued spacetime approximately by using shock waves for AdS JT gravity outlined in rection 6. This is closely related to the exact construction in section 3, but the resulting geometry does not have the time reflection symmetry $\tau \longleftrightarrow -\tau$[6].

At first, we consider the equations of motion (3.10) with the stress tensor given by

$$\langle T_{\pm\pm} \rangle = \langle T_{\pm\pm} \rangle_\beta + \langle T_{\pm\pm} \rangle_S, \quad \langle T_{\pm\mp} \rangle = 0, \tag{B.1}$$

where the first term $\langle T_{\pm\pm} \rangle_\beta$ is defined by (3.6) and the second term $\langle T_{\pm\pm} \rangle_S$ is coming from the contribution of the shock wave,

$$\langle T_{++} \rangle_S = E\delta(x^+ - x_0^+), \quad \langle T_{--} \rangle_S = 0. \tag{B.2}$$

Here, the coefficient E characterizes the strength of the shock wave and x_0^+ is the location of the shock wave.

The general solution is given by[7]

$$\Phi = b_+ \left(\frac{\cos \tau}{\cos \mu} \right) - 16\pi G \langle T \rangle_\beta (\mu \tan \mu + 1)$$

$$- 16\pi GE \cos^2 \left(\frac{x_0^+ + x^-}{2} \right) \left[\tan \mu - \tan \left(\frac{x_0^+ + x^-}{2} \right) \right] \Theta(x^+ - x_0^+). \tag{B.3}$$

As we will check in the next subsection, this dilaton profile corresponds to a black hole with two different masses. In other words, this dilaton profile describes a new glued spacetime with its masses.

B.1   Black hole ADM Mass formula in the AdS Jackiw-Teitelboim gravity

Next we compute the black hole masses described by the dilaton profile (B.3) by using the ADM mass formula (A.3).

---

[6]We can construct a dilaton profile describing a glued geometry which is not time reflection symmetric with the method discussed in section 3 by including the additional term in (3.10). See footnote footnote 3.

[7]Although the full general solution includes terms $\sin \tau / \cos \mu$ and $\tan \mu$, we omit such terms for simplicity.

To use the ADM black hole mass formula, we need to calculate the normal derivative of the dilaton $\partial_n \Phi$. After some algebras, we get

$$\partial_n \Phi = \Bigg[\Phi^2 - \Big\{ b_+ \left(b_+ + 16\pi GE \sin x_0^+ \Theta \left(x^+ - x_0^+ \right) \right) - 16\pi G \langle T \rangle_\beta \cdot 16\pi GE \cdot \mu \, \Theta \left(x^+ - x_0^+ \right)$$
$$- (16\pi G \langle T \rangle_\beta)^2 \cdot \mu^2 \Big\}$$
$$+ 16\pi G \langle T \rangle_\beta \cos \mu \Big\{ 2(b_+ + 8\pi GE \sin x_0^+ \Theta \left(x^+ - x_0^+ \right)) \cos t$$
$$- 16\pi GE \cos x_0^+ \sin t - 16\pi G \langle T \rangle_\beta \cos \mu \Big\} + \cdots \Bigg]^{\frac{1}{2}},$$
$$\text{(B.4)}$$

where the dots $\cdots$ denotes terms containing the delta function, which comes from the derivative of the step function $\Theta \left(x^+ - x_0^+ \right)$, and the terms do not contribute to the black hole mass and below we ignore such terms.

Therefore, from the ADM black hole mass formula (A.3) and the boundary conditions (A.1), (A.2), the black hole masses associated with two AdS boundaries are

$$M_{ADM,\mathrm{L}} = -\frac{\sqrt{-g_{uu}}}{8\pi G} (\partial_n \Phi - \Phi)|_{\mathrm{Left}\ bdy,\ \mu \to -\pi/2}$$
$$= \frac{1}{16\pi G \phi_b} \Big\{ b_+^2 - \left(8\pi^2 G \langle T \rangle_\beta \right)^2 \Big\}$$
$$\text{(B.5)}$$

and

$$M_{ADM,\mathrm{R}} = -\frac{\sqrt{-g_{uu}}}{8\pi G} (\partial_n \Phi - \Phi)|_{\mathrm{Right}\ bdy,\ \mu \to \pi/2}$$
$$= \frac{1}{16\pi G \phi_b} \Big\{ b_+ \left(b_+ + 16\pi GE \sin x_0^+ \right) - 128\pi^2 G^2 E \langle T \rangle_\beta - \left(8\pi^2 G \langle T \rangle_\beta \right)^2 \Big\}.$$
$$\text{(B.6)}$$

Since these ADS black hole masses associated with the dilaton profile (B.3) are clearly different $M_{ADM,\mathrm{L}} \neq M_{ADM,\mathrm{R}}$ unless $E = 0$, thus the dilaton profile (B.3) describes the glued geometry with different black hole masses $M_{ADM,\mathrm{L}}, M_{ADM,\mathrm{R}}$.

C The black hole solution with a shockwave in its interior (Flat CGHS gravity)

In this appendix, for CGHS gravity in flat spacetime, we explain a method to construct a dilaton profile describing a glued spacetime approximately by using a shock wave. The

discussion is parallel to the JT gravity case. This method is also closely related to the one in section 4, and the resulting geometry also does not have the time reflection symmetry $t \longleftrightarrow -t$ as in the case of JT gravity[8].

Firstly, we consider the equations of motion (4.2) with the stress energy tensor given by the previous one (B.1).

The full solution is given by[9]

$$
\begin{aligned}
\Phi = \phi_0 + \frac{|\Lambda|}{4} \tan x^+ \tan x^- &- 4\pi G \langle T \rangle_\beta (x^+ \tan x^+ + x^- \tan x^-) \\
&- 8\pi G E \cos^2 x_0^+ \left(\tan x^+ - \tan x_0^+ \right) \Theta(x^+ - x_0^+).
\end{aligned}
\tag{C.1}
$$

This dilaton profile (C.1) corresponds to a black hole with two different masses in CGHS gravity. In other words, this dilaton profile describes a new glued spacetime with its masses.

C.1   Black hole ADM Mass formula in CGHS gravity

Next we compute the black hole mass described by the dilaton profile (C.1) by using the ADM mass formula (A.6).

To use the ADM mass formula (A.6), we need to evaluate the factor $(\nabla \Phi)^2$, which is given by

$$
\begin{aligned}
(\nabla \Phi)^2 = 4 &\left[\frac{|\Lambda|}{4} \tan x^- - 4\pi G \langle T \rangle_\beta (\cos x^+ \sin x^+ + x^+) \right] \\
&\times \left[\frac{|\Lambda|}{4} \tan x^+ - 4\pi G \langle T \rangle_\beta (\cos x^- \sin x^- + x^-) \right] \\
&- 32\pi G E \cos^2 x_0^+ \left[\frac{|\Lambda|}{4} \tan x^+ - 4\pi G \langle T \rangle_\beta (\cos x^- \sin x^- + x^-) \right].
\end{aligned}
\tag{C.2}
$$

Thus the black hole masses at the left and right asymptotic spatial infinity are given by

$$
\begin{aligned}
M_{ADM,L} &= \lim_{x^\pm \to -\frac{\pi}{2}} \frac{1}{16\pi G \sqrt{|\Lambda|}} \left(-(\nabla \Phi)^2 + |\Lambda| \Phi \right) \\
&= \frac{\sqrt{|\Lambda|}}{16\pi G} \left\{ \phi_0 - \frac{\left(4\pi^2 G \langle T \rangle_\beta \right)^2}{|\Lambda|} \right\},
\end{aligned}
\tag{C.3}
$$

---

[8]In this case, we can also construct a glued geometry which is not time reflection symmetric with the method discussed in section 4 by considering $D^+ \neq D^-$ cases.

[9]The full general solution also includes terms $\tan x^+$ and $\tan x^-$, but we omit them for simplicity.

and

$$M_{ADM,\mathrm{R}} = \lim_{x^{\pm} \to \frac{\pi}{2}} \frac{1}{16\pi G\sqrt{|\Lambda|}} \left(-(\nabla\Phi)^2 + |\Lambda|\Phi \right)$$
$$= \frac{\sqrt{|\Lambda|}}{16\pi G} \left\{ \phi_0 - \frac{\left(4\pi^2 G\langle T\rangle_{\beta} \right)^2}{|\Lambda|} - \frac{64\pi^3 G^2 E\langle T\rangle_{\beta} \cos^2 x_0^+}{|\Lambda|} + 8\pi GE \cos x_0^+ \sin x_0^+ \right\}. \tag{C.4}$$

In this case, since the black hole masses $M_{ADM,\mathrm{L}}, M_{ADM,\mathrm{R}}$ are clearly different again, the dilaton profile (C.1) describes the black hole with two different black hole masses.

References

[1] S. W. Hawking, *Particle Creation by Black Holes*, *Commun. Math. Phys.* **43** (1975) 199.

[2] S. W. Hawking, *Breakdown of Predictability in Gravitational Collapse*, *Phys. Rev. D* **14** (1976) 2460.

[3] D. N. Page, *Information in black hole radiation*, *Phys. Rev. Lett.* **71** (1993) 3743 [hep-th/9306083].

[4] D. N. Page, *Time Dependence of Hawking Radiation Entropy*, *JCAP* **09** (2013) 028 [1301.4995].

[5] G. Penington, *Entanglement Wedge Reconstruction and the Information Paradox*, 1905.08255.

[6] A. Almheiri, N. Engelhardt, D. Marolf and H. Maxfield, *The entropy of bulk quantum fields and the entanglement wedge of an evaporating black hole*, *JHEP* **12** (2019) 063 [1905.08762].

[7] A. Almheiri, R. Mahajan, J. Maldacena and Y. Zhao, *The Page curve of Hawking radiation from semiclassical geometry*, *JHEP* **03** (2020) 149 [1908.10996].

[8] G. Penington, S. H. Shenker, D. Stanford and Z. Yang, *Replica wormholes and the black hole interior*, 1911.11977.

[9] A. Almheiri, T. Hartman, J. Maldacena, E. Shaghoulian and A. Tajdini, *Replica Wormholes and the Entropy of Hawking Radiation*, *JHEP* **05** (2020) 013 [1911.12333].

[10] M. Rozali, J. Sully, M. Van Raamsdonk, C. Waddell and D. Wakeham, *Information radiation in BCFT models of black holes*, 1910.12836.

[11] H. Z. Chen, Z. Fisher, J. Hernandez, R. C. Myers and S.-M. Ruan, *Information Flow in Black Hole Evaporation*, *JHEP* **03** (2020) 152 [1911.03402].

[12] R. Bousso and M. Tomašević, *Unitarity From a Smooth Horizon?*, *Phys. Rev. D* **102** (2020) 106019 [1911.06305].

[13] A. Almheiri, R. Mahajan and J. E. Santos, *Entanglement islands in higher dimensions*, 1911.09666.

[14] Y. Chen, *Pulling Out the Island with Modular Flow*, 1912.02210.

[15] V. Balasubramanian, A. Kar, O. Parrikar, G. Sárosi and T. Ugajin, *Geometric secret sharing in a model of Hawking radiation*, 2003.05448.

[16] T. J. Hollowood and S. P. Kumar, *Islands and Page Curves for Evaporating Black Holes in JT Gravity*, 2004.14944.

[17] M. Alishahiha, A. Faraji Astaneh and A. Naseh, *Island in the presence of higher derivative terms*, *JHEP* **02** (2021) 035 [2005.08715].

[18] H. Z. Chen, R. C. Myers, D. Neuenfeld, I. A. Reyes and J. Sandor, *Quantum Extremal Islands Made Easy, Part I: Entanglement on the Brane*, 2006.04851.

[19] H. Geng and A. Karch, *Massive Islands*, 2006.02438.

[20] V. Chandrasekaran, M. Miyaji and P. Rath, *Including contributions from entanglement islands to the reflected entropy*, *Phys. Rev. D* **102** (2020) 086009 [2006.10754].

[21] T. Li, J. Chu and Y. Zhou, *Reflected Entropy for an Evaporating Black Hole*, *JHEP* **11** (2020) 155 [2006.10846].

[22] R. Bousso and E. Wildenhain, *Gravity/ensemble duality*, *Phys. Rev. D* **102** (2020) 066005 [2006.16289].

[23] X. Dong, X.-L. Qi, Z. Shangnan and Z. Yang, *Effective entropy of quantum fields coupled with gravity*, 2007.02987.

[24] T. J. Hollowood, S. Prem Kumar and A. Legramandi, *Hawking radiation correlations of evaporating black holes in JT gravity*, *J. Phys. A* **53** (2020) 475401 [2007.04877].

[25] H. Z. Chen, Z. Fisher, J. Hernandez, R. C. Myers and S.-M. Ruan, *Evaporating Black Holes Coupled to a Thermal Bath*, *JHEP* **01** (2021) 065 [2007.11658].

[26] Y. Chen, V. Gorbenko and J. Maldacena, *Bra-ket wormholes in gravitationally prepared states*, 2007.16091.

[27] T. Hartman, Y. Jiang and E. Shaghoulian, *Islands in cosmology*, 2008.01022.

[28] V. Balasubramanian, A. Kar and T. Ugajin, *Entanglement between two disjoint universes*, *JHEP* **02** (2021) 136 [2008.05274].

[29] V. Balasubramanian, A. Kar and T. Ugajin, *Islands in de Sitter space*, *JHEP* **02** (2021) 072 [2008.05275].

[30] Y. Ling, Y. Liu and Z.-Y. Xian, *Island in Charged Black Holes*, *JHEP* **03** (2021) 251 [2010.00037].

[31] H. Z. Chen, R. C. Myers, D. Neuenfeld, I. A. Reyes and J. Sandor, *Quantum Extremal Islands Made Easy, Part II: Black Holes on the Brane*, *JHEP* **12** (2020) 025 [2010.00018].

[32] A. Bhattacharya, A. Chanda, S. Maulik, C. Northe and S. Roy, *Topological shadows and complexity of islands in multiboundary wormholes*, *JHEP* **02** (2021) 152 [2010.04134].

[33] D. Harlow and E. Shaghoulian, *Global symmetry, Euclidean gravity, and the black hole information problem*, *JHEP* **04** (2021) 175 [2010.10539].

[34] I. Akal, *Universality, intertwiners and black hole information*, 2010.12565.

[35] J. Hernandez, R. C. Myers and S.-M. Ruan, *Quantum extremal islands made easy. Part III. Complexity on the brane*, *JHEP* **02** (2021) 173 [2010.16398].

[36] Y. Matsuo, *Islands and stretched horizon*, 2011.08814.

[37] I. Akal, Y. Kusuki, N. Shiba, T. Takayanagi and Z. Wei, *Entanglement Entropy in a Holographic Moving Mirror and the Page Curve*, *Phys. Rev. Lett.* **126** (2021) 061604 [2011.12005].

[38] T. Numasawa, *Four coupled SYK models and Nearly AdS$_2$ gravities: Phase Transitions in Traversable wormholes and in Bra-ket wormholes*, 2011.12962.

[39] J. Kumar Basak, D. Basu, V. Malvimat, H. Parihar and G. Sengupta, *Islands for Entanglement Negativity*, 2012.03983.

[40] H. Geng, A. Karch, C. Perez-Pardavila, S. Raju, L. Randall, M. Riojas et al., *Information Transfer with a Gravitating Bath*, 2012.04671.

[41] F. Deng, J. Chu and Y. Zhou, *Defect extremal surface as the holographic counterpart of Island formula*, *JHEP* **03** (2021) 008 [2012.07612].

[42] G. K. Karananas, A. Kehagias and J. Taskas, *Islands in Linear Dilaton Black Holes*, 2101.00024.

[43] X. Wang, R. Li and J. Wang, *Islands and Page curves of Reissner-Nordström black holes*, *JHEP* **04** (2021) 103 [2101.06867].

[44] K. Kawabata, T. Nishioka, Y. Okuyama and K. Watanabe, *Probing Hawking radiation through capacity of entanglement*, 2102.02425.

[45] S. Fallows and S. F. Ross, *Islands and mixed states in closed universes*, 2103.14364.

[46] A. Bhattacharya, A. Bhattacharyya, P. Nandy and A. K. Patra, *Islands and complexity of eternal black hole and radiation subsystems for a doubly holographic model*, *JHEP* **05** (2021) 135 [2103.15852].

[47] W. Kim and M. Nam, *Entanglement entropy of asymptotically flat non-extremal and extremal black holes with an island*, *Eur. Phys. J. C* **81** (2021) 869 [2103.16163].

[48] L. Anderson, O. Parrikar and R. M. Soni, *Islands with Gravitating Baths*, 2103.14746.

[49] A. Miyata and T. Ugajin, *Evaporation of black holes in flat space entangled with an auxiliary universe*, 2104.00183.

[50] X. Wang, R. Li and J. Wang, *Islands and Page curves for a family of exactly solvable evaporating black holes*, 2104.00224.

[51] K. Ghosh and C. Krishnan, *Dirichlet baths and the not-so-fine-grained Page curve*, *JHEP* **08** (2021) 119 [2103.17253].

[52] L. Aalsma and W. Sybesma, *The Price of Curiosity: Information Recovery in de Sitter Space*, 2104.00006.

[53] H. Geng, S. Lüst, R. K. Mishra and D. Wakeham, *Holographic BCFTs and Communicating Black Holes*, 2104.07039.

[54] V. Balasubramanian, A. Kar and T. Ugajin, *Entanglement between two gravitating universes*, 2104.13383.

[55] C. F. Uhlemann, *Islands and Page curves in 4d from Type IIB*, *JHEP* **08** (2021) 104 [2105.00008].

[56] X.-L. Qi, *Entanglement island, miracle operators and the firewall*, 2105.06579.

[57] K. Kawabata, T. Nishioka, Y. Okuyama and K. Watanabe, *Replica wormholes and capacity of entanglement*, *JHEP* **10** (2021) 227 [2105.08396].

[58] J. Chu, F. Deng and Y. Zhou, *Page curve from defect extremal surface and island in higher dimensions*, *JHEP* **10** (2021) 149 [2105.09106].

[59] K. Langhoff, C. Murdia and Y. Nomura, *Multiverse in an inverted island*, *Phys. Rev. D* **104** (2021) 086007 [2106.05271].

[60] Y. Lu and J. Lin, *Islands in Kaluza-Klein black holes*, 2106.07845.

[61] I. Akal, Y. Kusuki, N. Shiba, T. Takayanagi and Z. Wei, *Holographic moving mirrors*, *Class. Quant. Grav.* **38** (2021) 224001 [2106.11179].

[62] V. Balasubramanian, B. Craps, M. Khramtsov and E. Shaghoulian, *Submerging islands through thermalization*, *JHEP* **10** (2021) 048 [2107.14746].

[63] B. Ahn, S.-E. Bak, H.-S. Jeong, K.-Y. Kim and Y.-W. Sun, *Islands in charged linear dilaton black holes*, 2107.07444.

[64] M. Miyaji, *Island for Gravitationally Prepared State and Pseudo Entanglement Wedge*, 2109.03830.

[65] Y. Matsuo, *Entanglement entropy and vacuum states in Schwarzschild geometry*, 2110.13898.

[66] Y. Chen and H. W. Lin, *Signatures of global symmetry violation in relative entropies and replica wormholes*, *JHEP* **03** (2021) 040 [2011.06005].

[67] P.-S. Hsin, L. V. Iliesiu and Z. Yang, *A violation of global symmetries from replica wormholes and the fate of black hole remnants*, 2011.09444.

[68] N. Engelhardt, S. Fischetti and A. Maloney, *Free energy from replica wormholes*, *Phys. Rev. D* **103** (2021) 046021 [2007.07444].

[69] A. Karlsson, *Replica wormhole and island incompatibility with monogamy of entanglement*, 2007.10523.

[70] K. Goto, T. Hartman and A. Tajdini, *Replica wormholes for an evaporating 2D black hole*, 2011.09043.

[71] S. Hirano and T. Kuroki, *Replica Wormholes from Liouville Theory*, 2109.12539.

[72] X. Dong, S. McBride and W. W. Weng, *Replica Wormholes and Holographic Entanglement Negativity*, 2110.11947.

[73] A. Almheiri, R. Mahajan and J. Maldacena, *Islands outside the horizon*, 1910.11077.

[74] W. Donnelly and L. Freidel, *Local subsystems in gauge theory and gravity*, *JHEP* **09** (2016) 102 [1601.04744].

[75] S. Raju, *Failure of the split property in gravity and the information paradox*, 2110.05470.

[76] J. Maldacena and L. Susskind, *Cool horizons for entangled black holes*, *Fortsch. Phys.* **61** (2013) 781 [1306.0533].

[77] A. Lewkowycz and J. Maldacena, *Generalized gravitational entropy*, *JHEP* **08** (2013) 090 [1304.4926].

[78] A. Goel, H. T. Lam, G. J. Turiaci and H. Verlinde, *Expanding the Black Hole Interior: Partially Entangled Thermal States in SYK*, *JHEP* **02** (2019) 156 [1807.03916].

[79] N. Iizuka, A. Miyata and T. Ugajin, *A comment on a fine-grained description of evaporating black holes with baby universes*, 2111.07107.

[80] Y. Nomura, *Reanalyzing an Evaporating Black Hole*, *Phys. Rev. D* **99** (2019) 086004 [1810.09453].

[81] J. Maldacena, D. Stanford and Z. Yang, *Conformal symmetry and its breaking in two dimensional Nearly Anti-de-Sitter space*, *PTEP* **2016** (2016) 12C104 [1606.01857].

[82] D. Harlow and D. Jafferis, *The Factorization Problem in Jackiw-Teitelboim Gravity*, *JHEP* **02** (2020) 177 [1804.01081].

[83] M. Cadoni, *Trace anomaly and Hawking effect in generic 2-D dilaton gravity theories*, *Phys. Rev. D* **53** (1996) 4413 [gr-qc/9510012].

[84] R. B. Mann, *Conservation laws and 2-D black holes in dilaton gravity*, *Phys. Rev. D* **47** (1993) 4438 [hep-th/9206044].